Marine Corrosion Mitigation of Mild Steel in Simulated Sea Water by Leaf Extract of *Barteria Fistulosa*

K. D. Ogwo [1,*], L. A. Nnanna [2], A. E. Emea[3], U. Joseph[2], A. C. Young[4]

[1] Physics Department, College of Basic and Applied Sciences, Rhema University, Aba, Nigeria.

[2] Physics Department, Michael Okpara University of Agriculture, Umudike, Nigeria.

[3] Physics Department, Clifford University, Owerrinta, Abia State.

[4]Physics Department, Gregory University, Uturu, Abia State.

ABSTRACT: Carbon steel is one of the major materials used in the construction of sea piers as well as oil and gas transit pipes. The corrosion of undersea oil and gas pipelines often lead to leakages which result in financial losses and irreparable damage to marine lives. The aim of this study was to investigate marine corrosion mitigation of mild steel in simulated sea water by leaf extract of Barteria fistulosa. The study investigated the use of *Barteria fistulosa* (BF) leaves extract as a non-toxic corrosion inhibitor of low carbon steel in 3.5% NaCl employing weight loss method, potentiodynamic polarization (PDP) and electrochemical impedance spectroscopy (EIS). The weight loss result indicated a significant drop in metal corrosion upon the introduction of the leaves extract to the salt solution. The correlation coefficient (R^2) values obtained from isotherm study showed that Langmuir model best fitted the inhibitor extract adsorption on the metal surface. The values of the Gibb's free energy of adsorption (ΔG_{ads}) were negative and ranges between -17 to -9 kJ/mol. This indicates that the adsorption process of the leaves extract is both spontaneous and physical. The weight-loss, PDP and EIS results all showed incremental change in efficiency of the inhibitor as its concentration is raised. This reveals that BF leaves extracts offered a shield to low carbon steel in the simulated sea water environment.

KEYWORDS: *Barteria fistulosa*, isotherm, efficiency, low carbon steel, corrosion

[Received Feb. 22, 2025; Revised Apr 03, 2025; Accepted Dec 05, 2025] Print ISSN: 0189-9546 | Online ISSN: 2437-2110

I. INTRODUCTION

Low carbon steel is a low-cost metallic alloy whose physical properties encourage its use in the construction of desalination plants, piers, oil and gas pipelines as well as body parts of ships. Undersea pipelines and sea vessels usually undergo electrochemical degradation due to periodic interaction with seawater chloride ions and dissolved oxygen (Fatah *et al.*, 2019; Hussein *et al.*, 2023). Unchecked corrosion can lead to fissures in oil and gas transit pipes which result in leakage of the transported product (Song *et al.*, 2023). Aside the financial losses incurred from oil spillage, the damages caused to marine lives are sometimes irreversible (McGenity *et al.*, 2012; Akpan, 2022). More so, the collapse of marine bridges and seaport piers due to pressure from tidal waves can be attributed to the failure of concrete or steel supports that has been weakened by corrosion (Menga *et al.*, 2022).

In recent times, plant extracts (Ogwo *et al.*, 2024a), barrier coatings (George, 2022), electroplating (Cao *et al.*, 2024), and cathodic protection (Mobin and Zehra, 2023) have been used to check corrosion. In corrosion control, environmental and ecological preservation is a major consideration due to the toxic nature of some corrosion inhibitors. However, the low-toxicity, cost effectiveness, and biodegradable nature of plant extracts or organic inhibitors make it one of the most preferred methods of mitigating corrosion in industries (Zakeri *et al.*, 2022). Plant extracts capable of retarding corrosion contain bioactive organic species (alkaloids, tannins, carbohydrates) which possess aromatic rings and a heterocyclic structure that serves as adsorption center (Sheetal *et al.*, 2023). Organic inhibitor molecules could either be physically assimilated on the metal surface by ionic interaction between the adsorbent and adsorbate or chemically assimilated by an electron transfer process (Kachel *et al.*, 2020).

There exist numerous scientific studies on the corrosion mitigation properties of plant extracts on low carbon steel (mild steel) in saline medium. Some plant extracts that have been investigated as corrosion inhibitor of mild steel in salt water include; N*ymphae pubens* leaf (Kalada *et al.*, 2017), Rice straw (Othman *et al.*, 2019), *Spondias mombin* Leaves (Ogwo *et al*, 2023), *Anacardium occidentale* leaf (Ezzat *et al,* 2024),

*Corresponding author: ogwo.dede@rhemauniversity.edu.ng ***doi:****http://doi.org/10.63746/njtd.v22i5.3429*

and *Allium sativum* (Devikala, 2019). These plant extracts were found to retard the dissolution of mild steel in NaCl solutions. The inhibition capabilities of these extracts can be credited to the presence hetero-atoms which occludes the active sites prone to corrosion (Casteneda *et al.,* 2008).

The aim of this study is to investigate the efficacy of *Barteria fistulosa* (BF) leaf extracts as an economically viable and ecologically sound corrosion inhibitor of low carbon steel in 3.5 wt.% NaCl. In this simulation study, weight-loss measurements were done at room temperature, as well as 45^0 and 60^0. Room temperature was considered because it is the established standard weather condition and can be easily controlled. The elevated temperatures (45^0C and 60^0C) were chosen to make accommodation for extreme temperature rise.

Barteria fistulosa belongs to the *passifloraceae* plant family which has been reported to contain cyanoheterosides, alkaloids, flavonoids, terpenoids, and tannins phytochemicals (Ingale and Hivrale, 2010). *BF* leaf extracts have been reported to inhibit the corrosion of AA2024 aluminium alloy in 3.5 wt% NaCl (Ogwo *et al.*, 2024b). According to this study, *BF* was found to lessen the rate of AA2024 deterioration in the NaCl solution. The ability of *BF* leaf extracts to retard metal dissolution could possibly be credited to the nature of the aggressive environment or the metal being investigated. This observation encouraged the investigation of the selected leaves extract as a corrosion inhibitor of mild steel in saline solution using weight loss, potentiodynamic polarization (PDP), and electrochemical impedance spectroscopy (EIS) methods.

II. MATERIALS AND METHODS

Ethanol extract of *Barteria fistulosa* (BF) leaves was investigated as corrosion inhibitor in a weight loss, polarization (PDP), and electrochemical impedance spectroscopy (EIS) experiments. The effect of temperature on the inhibitor's efficacy was studied by varying the temperature of the test solutions. Different isotherm model was employed to understand the adsorption mechanism of the leaf extract on the mild steel surface.

A. Materials

The materials used include; Barteria fistulosa leaves, low carbon steel coupons, distilled water, NaCl, acetone, Nitirc acid, ethanol, Soxlet extractor, emery paper, VersaSTAT 400 DC Voltametry system, and electronic weighing balance (LAB300).

B. Methods

1) Preparation of test solution

Every chemical solution used in the experiment is of analytical grade. Fresh *Barteria fistulosa* leaves were obtained from *New Market*, Aba, Nigeria. The leaves were washed, air dried and grounded into fine powder. A cellulose thimble with dimensions of 28 x 80 cm filled with 0.05 kg mass of the ground leaves was placed in Soxhlet extractor containing 150 mL ethanol solution. Heat supplied by the heating mantle causes the ethanol to vaporize as it boils. As the vaporized ethanol rises through the Soxlet arm, its temperature drops, which makes it to condense as droplets into the thimble. As a result, a mixture consisting of both the leaves extract and ethanol was formed. This mixture was refluxed for 2.5 hours before the concentrated solution containing the extracts was evaporated at a temperature of 78.5^0C (ethanol's boiling point) to obtain a dark brown semi solid substance. Subsequently, different masses of the extracts were measured and then mixed with the solution containing the required weight percentage (3.5%) NaCl.

2) Preparation of metal

The low carbon steel used for this experiment was obtained from Federal University of Petroleum Resources, Effurun, Nigeria. The elemental composition of the mild steel is as follows: 96.56 % Fe, 0.05 % C, 0.85 % P, 0.15 % Pb, 0.09 % Cu, 1.13 % Mn, 0.85 % S, 0.13 % V, 0.08 % Mo and 0.05 % Si. The metal alloy was press cut to a dimension of 1.5 cm x 1.5 cm. The coupons were polished mechanically with emery paper of different grades, degreased in ethanol, washed with distilled water, air dried and then stored in moisture free environment. Accurate triplicate weight measurements of the coupons were taken using electronic weighing balance.

3) Weight loss measurements

Triplicate pre-weighed metal coupons were dipped in 3.5% wt NaCl solutions containing 0 to 0.5 g doses of the leaf extracts at room temperature. The submerged samples were periodically removed from the aggressive saline solution at intervals 2 hours for 10 hours exposure time. The retrieved metals were washed, air dried, and re-weighed to obtain the final weight. The experiments were repeated at higher temperatures of 45^0C and 60 ^{0}C. The weight loss of each retrieved sample was calculated by taking the difference between its weight before immersion and the weight after immersion. The data obtained from the weight loss experiment were used to calculate the corrosion rates (*C.R*) of the samples, inhibition efficiencies (*%*) of the leaf extracts, and surface coverage (θ) using equations 1, 2 and 3 respectively.

$$C.R = \frac{k\Delta w}{\rho A t} \quad (1)$$

Where ΔW is the weight loss (in g), ρ is the density of sample (in g/cm^3), A is the area of sample in cm^2, t is the time of exposure in hours.

$$I(\%) = \left(1 - \frac{\rho_1}{\rho_0}\right) 100\ \% \quad (2)$$

Where ρ_1 and ρ_0 are the corrosion rate in the presence and absence of the leaf extracts respectively.

$$\theta = \frac{\rho_0 - \rho_1}{\rho_0} \quad (3)$$

4) Isotherm studies

The isotherm study is mostly employed to investigate the mode and nature of interaction between the inhibitor molecules and the metal surface under a temperature-controlled environment. The adsorption

behaviour of *Barteria fistulosa* leaves extract on carbon steel was studied by fitting data obtained from the weight loss measurements into different adsorption isotherms which include: Langmuir, Temkin, and Freundlich isotherms represented by Equations 1, 2 and 3 respectively.

$$\frac{C}{\theta} = \frac{1}{K_{ads}} + C \quad (4)$$

Where Θ is the surface coverage, C is the inhibitor concentration and K_{ads} is the equilibrium constant of the adsorption process.

$$\theta = \frac{1}{f} Ink_{ads} + \frac{1}{f} InC \quad (5)$$

where, f determines the extract's molecule and metal surface interaction.

$$\log\theta = \log k + n\log C \quad (6)$$

Where the constant "n" describes the adsorption intensity of the leaves extract.

The equilibrium constant (K_{ads}) is employed in calculating Gibb's free energy of adsorption (ΔG^0_{ads}).

$$\Delta G_{ads} = -RT\, In(55.5K_{ads}) \quad (7)$$

Where T is the temperature in kelvin, and R is the universal gas constant in $kJmol^{-1}$.

5) Electrochemical Measurements

The electrochemical measurement (PDP and EIS) was performed at room temperature using triple electrode configuration system. Saturated calomel was used as reference electrode while low carbon steel coupon and platinum plate of 1.5 cm^2 surface area were employed as the working and counter electrode respectively. The working electrode is needed for current measurement and potential regulation. The reference electrode which is maintained at same potential is required to measure the potential of the working electrode. The electrodes were partly immersed in 3.5 wt% NaCl test solutions containing 0, 100, 500 and 1000 mg/L of the leaves extract. In order to attain stability at open circuit potential (OCP), potential pulse was applied to the electrodes through the potentiostat for a period of 30 minutes. The system was further subjected to a controlled scan speed of 0.15 mV/s within a potential range of ± 0.25 V. The potentiostat was used to measure the current density as the potential navigate from the anodic to the cathodic direction.

The EIS measurements were performed over a frequency spectrum of 10 Hz to 100 kHz at room temperature using ± 5 mV amplitude signals at the established OCP. EC301 Potentiostat connected to an SRSLab application was used to analyze the impedance spectroscopy data. To accomplish reproducibility, the experiments were done in triplicate. The inhibition efficiencies of the leaf extract for the PDP and EIS experiments were calculated using equation (8) and (9) respectively.

$$IE = 1 - \frac{i^{in}_{corr}}{i^{0}_{corr}} \times 100 \quad (8)$$

Where i^0_{corr} is the corrosion current density for the blank solution and i^{in}_{corr} is the corrosion current density for the inhibited system.

$$IE = 1 - \frac{R^0_{ct}}{R^{in}_{ct}} \times 100 \quad (9)$$

Where R^0_{ct} is the charge transfer resistance for the blank solution and R^{in}_{ct} is the charge transfer resistance for the inhibited system.

III. RESULTS AND DISCUSSION

A. Weight loss analysis

The plot of the corrosion rates of low carbon steel versus the leaf extracts concentration after 8 hours of exposure is shown in figure 1. The graph shows a decline in the rate of metal dissolution with increasing concentration of the leaf extracts but an increase in corrosion rate as temperature is elevated. For the blank saline environment, the metal samples

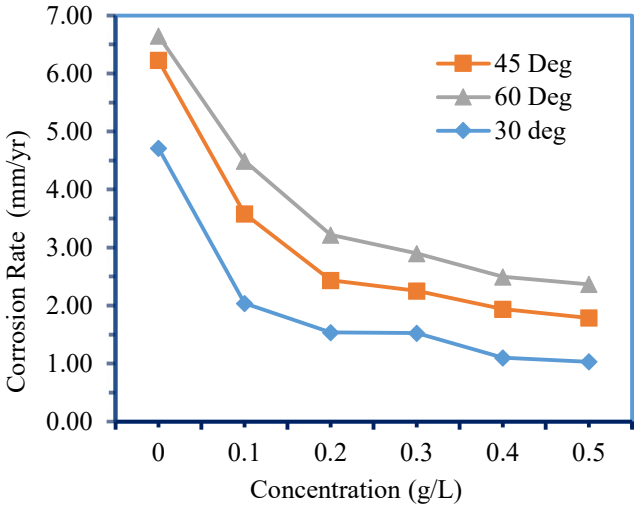

Figure 1 Plot of corrosion rate against concentration at various temp.

decayed at a high rate reaching 4.714 mm/yr at 30 ^{0}C, 6.230 mm/yr at 45 ^{0}C and 6.651 mm/yr at 60 ^{0}C temperatures.

However, for the samples immersed in solutions containing 0.5 g/L of the inhibitor, the corrosion rate diminished to 1.034 mm/yr at 30 ^{0}C, 1.788 mm/yr at 45 ^{0}C and 2.368 mm/yr at 60 ^{0}C temperatures. This diminishing corrosion rates indicate the assimilation of the leaf extract molecules which results to the development of a protective thin film on the metal's surface (Chaudhary and Tak, 2022). The plot of the inhibition efficiency versus inhibitor concentration is shown in Figure 2. The plot shows a significant rise in efficiency of the leaf extracts as its concentration is increased, suggesting a decline of metal dissolution into ions. However,

the inhibition efficiency decreased with temperature rise. At 0.5 g/l, optimum inhibition efficiency of 78.06%, 62.72 % and 54.85% were obtained at temperature of 30, 45, and 60 ^{0}C respectively. This decline in efficiency at elevated temperature is suggestive of physical adsorption of the leaf extracts molecules on the metals surface (Solmaz *et al*, 2022).

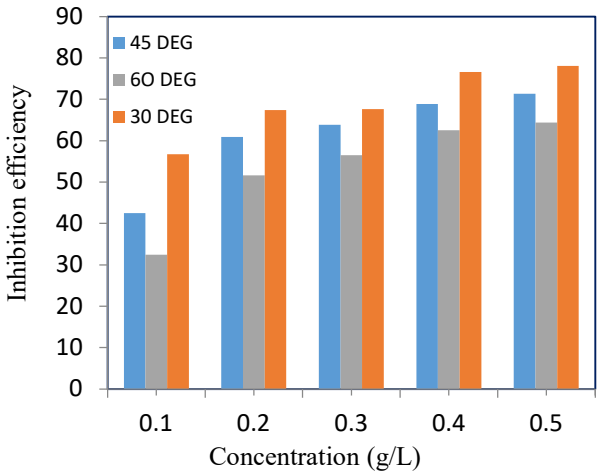

Figure 2 Plot of inhibition eff. against conc. at various temp.

B. Isotherm studies

Langmuir, Temkin, and Freundlich isotherm models were employed to analyze the nature of interaction between the adsorbate and the metal's surface. The adsorption isotherm plots obtained from the weight loss data is presented in figure 3a, b, and c. The adsorption parameters extracted from the isotherm plots are shown in Table 1. The isotherm model whose correlation coefficient (R^2) value is closest to unity is taken to be the most appropriate for the adsorption study (Ibrahim *et al*, 2023). Table 1 shows an average R^2 value of 0.994, 0.954, and 0.936 for Langmuir, Temkin, and Freundlich models respectively. The R^2 values revealed that Langmuir isotherm best fitted the inhibitor extract adsorption on the metal surface compared to the Temkin, and Freundlich models. This suggests that the leaves extract is adsorbed as a lone layer on the metal's surface (Ayawei *et al*, 2017). The limitation of lone layer adsorption is that it is surface oriented and weakens at elevated temperature. In all cases, the values of the Gibb's free energy of adsorption (ΔG_{ads}) were negative and ranges between -17 to -9 kJ/mol. This indicates that the adsorption process of the leaves extract is both spontaneous (Haldhar *et al*., 2021) and physical (Lai *et al*, 2017). The values adsorbent-adsorbate relation term "a" obtained from the Temkin plots were positive and less than unity ($0 < a < 1$). This suggests the existence of a bonding force acting parallel to metal-solution interface.

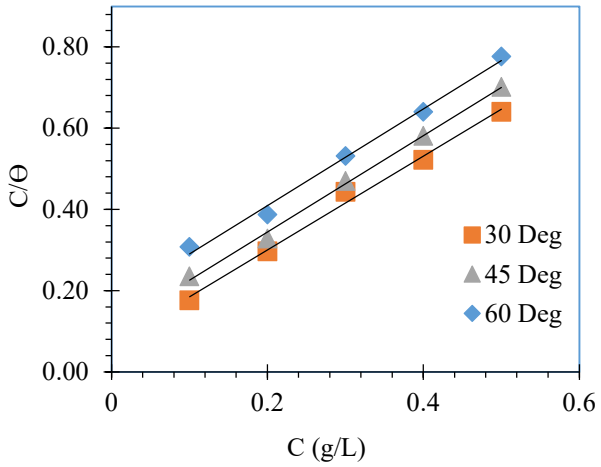

a. Langmuir adsorption isotherms plot

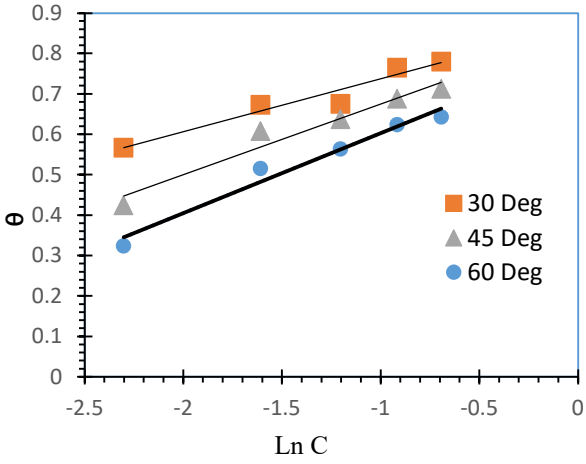

b. Temkin Isotherm plots

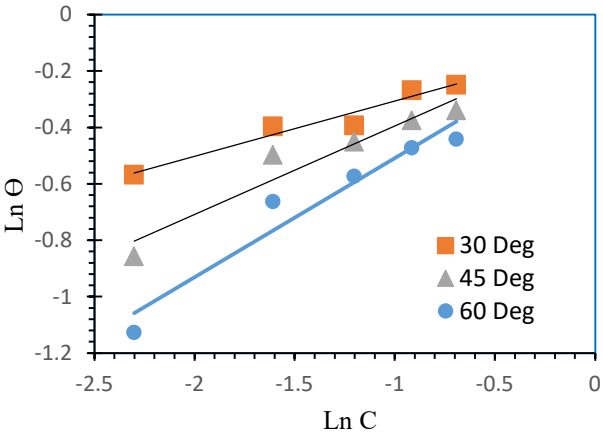

c. Freundlich Isotherm plots

Figure 3 Isotherm plots

Table 1: Adsorption isotherm parameters of *Barteria fistulosa* leaves extract on mild steel

	Langmuir			Temkin				Freundlich			
T (K)	**R^2**	**K_{ads}**	**ΔG_{ads} (kJ/mol)**	**R^2**	**a**	**K_{ads}**	**ΔG_{ads} (kJ/mol)**	**R^2**	**n**	**K_{ads}**	**ΔG_{ads} (kJ/mol)**
303	0.992	14.49	-16.8	0.940	0.06	1.11	-10.4	0.946	5.12	0.89	-9.8
318	0.997	9.34	-16.5	0.954	0.08	1.15	-11.0	0.927	3.19	0.92	-10.4
348	0.993	5.84	-16.0	0.969	0.09	1.17	-11.5	0.936	2.36	0.91	-10.8

C. Electrochemical Measurement

1) Electrochemical Impedance Spectroscopy (EIS) Result

The Nyquist plot of mild steel exposed to 3.5% NaCl environment in the presence and absence *Barteria fistulosa* (BF) is shown in Figure 4. The Nyquist plot features semi-circular arcs ranging from high to low frequency. It can be observed from the plot that there is a radial increase of the loops as the concentration of the inhibitor is increased. This increase in arc radius is associated with rise in electron transfer resistance which opposes charge migration from the metal to the aggressive electrolyte leading to decline in corrosion (Feliu, 2020).

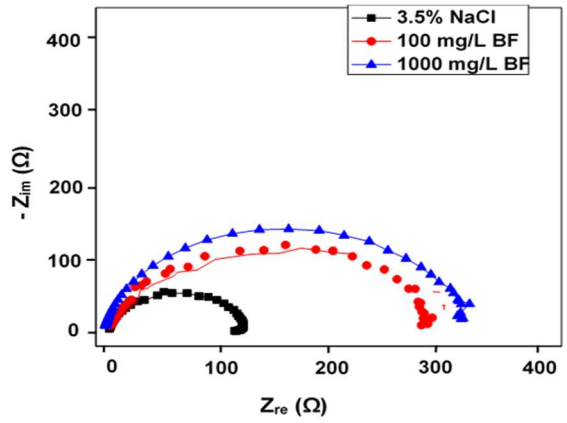

Figure 4 Nyquist plot of carbon steel in 3.5% NaCl

The impedance characteristics of the system was studied using equivalent circuit model as shown in Figure 5. The EIS equivalent circuit features the charge transfer resistance (R_{ct}), the solution resistance (R_s), dual-layer pure capacitor (C_{dl}) and surface roughness factor (n). R_{ct} depends on surface homogeneity of metal. Rough surfaces have high R_{ct} compared to smooth surfaces (Paswan *et al*., 2023). More so, Low R_{ct} value is associated with increased dissolution rate of metal while high values of R_{ct} imply that corrosion rate has been impeded (Zhai *et al.*, 2023).

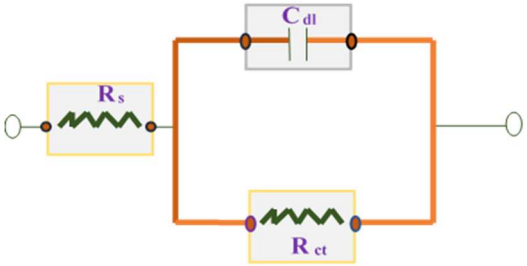

Figure 5 EIS Equivalent Model **Circuit**

Extrapolated EIS parameters are presented in Table 2. The table shows R_{ct} value of 105.3 Ω-cm^2 for the blank solution. However, for the inhibited environment, the R_{ct} value increased to 293.2 and 315.6 Ω-cm^2 at inhibitor concentration of 100 and 1000 mg/L respectively. The incremental change in R_{ct} suggest the formation of a tenuous film at the metal-solution interface (Liu *et al*, 2023). The dual-layer of the pure capacitor serves as a barrier which oppose ion migration between metal and the aggressive solution (Jeanmairet *et al*, 2022). The width of the double layer is modelled after the thickness of the surface protective film. The capacitance (C_{dl}) varies inversely with the thickness double-layer and as a result, decrease in C_{dl} value is associated with decline in metal degradation (Chidiebere *et al*, 2016; Nunez, 2024). The reported values of C_{dl} were found to decrease with rise in concentration of the inhibitor. This indicate that the assimilation of the leaves extract on the metal surface occluded the active corrosion sites. Table 2 also reveals that inhibition efficiency values of 64.1% and 66.7% was respectively obtained for 100 mg/L and 1000 mg/L concentration of BF leaves extract.

Table 2 EIS Parameters for low carbon steel in 3.5% NaCl solution in the Absence and Presence *Bateria fistulosa*

Conc. (mg/L)	n	R_s (Ω-cm^2)	R_{ct} (Ω-cm^2)	C_{dl} ($\mu\Omega^{-1}S^n cm^{-2}$) x$10^{-5}$	I.E. %
Blank	0.89	2.05	105.3	2.361	-
100	0.89	2.31	293.2	0.590	64.1
1000	0.88	1.80	315.6	0.684	66.7

Table 3 PDP Parameters for low carbon steel in 3.5% NaCl solution in the Absence and Presence *Bateria fistulosa*

Conc. (mg/L)	E_{corr} (mV vs SCE)	I_{corr} (μA/cm^2)	β_a (mV/dec)	$-\beta_c$ (mV/dec)	I.E%
Blank	-485.6	107.5	63.7	155.2	-
100	-491.4	32.4	60.1	147.0	64.1
1000	-483.2	29.7	76.4	153.5	66.7

2) Potentiodynamic Polarization Result

The effect of the leaves extracts on the cathodic and anodic reactions was studied using PDP measurements. The anodic reaction is associated with the dissociation of electron into the electrolyte (Bouguezzi *et al*, 2024) while the cathodic reaction involves the interaction of free electrons with water and free oxygen (Li *et al*, 2010). Cathodic and anodic reaction can be retarded by the addition of small amount of corrosion inhibitor (Al-Amiery *et al*, 2023). The polarization plot (Tafel curve) of low carbon steel exposed to 3.5% NaCl solution containing 0 mg/L to 1000 mg/L of the leaves extracts is displayed in figure 6.

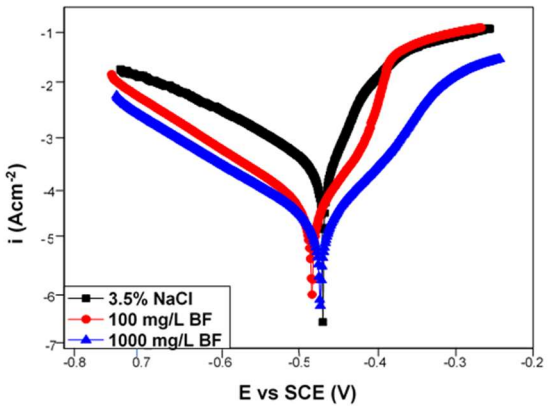

Figure 6 PDP Tafel plot of mild steel in 3.5 % NaCl

The plot (Figure 6) shows graph of current density (i) against potential (E). The corrosion current density (i_{corr}) corresponds to the meeting point of the linear slopes (β_c and β_a) of the Tafel curves. At this point, both anodic and cathodic reaction is known to proceed at the same rate (Rybalka *et al.*, 2021). The corrosion potential (E_{corr}) is the potential at open circuit. The Tafel plot shows that the leaves extracts had negligible effect on E_{corr}. The Extrapolated values of i_{corr} and E_{corr} is shown in Table 3. It can be observed that the addition of the inhibitor causes a significant drop in i_{corr} values. The lowered i_{corr} values implies that both the cathodic and anodic reactions were impeded. This feature is similar to that exhibited by inhibitors of mixed-type (Shwetha, *et al*., 2024). More so, drop in i_{corr} values corresponds to the shift of the curves toward lesser current density values as seen in Figure 6. The decline in i_{corr} values indicates retardation of metal corrosion rate which is in agreement with the weight loss and EIS results.

IV. CONCLUSION

The presence of the leaves extract of *Barteria fistulosa* significantly lowered the dissolution rate of low carbon steel in 3.5% NaCl. The weight loss result showed a decline in corrosion rate as the extracts concentration were increased. However, the efficacy of the leave extract lessened with rise in temperature of the inhibited environment. The PDP result indicated that the presence of the leaves extract limited the anodic and cathodic reactions. This implies that the extracts functions as inhibitor of mixed-type. The EIS data showed that the introduction of the extracts into the salt solution led to rise in charge transfer resistance (R_{ct}) and a corresponding depreciation in corrosion rate. This suggests the development of a film barrier at the metal-electrolyte boundary. The Langmuir, Temkin and Freundlich isotherm study showed that the obtained correlation coefficient values (R^2) were all close to unity. However, R^2 values revealed that Langmuir isotherm best fitted the inhibitor extract adsorption on the metal surface compared to the Temkin, and Freundlich models. The values of the Gibb's free energy of adsorption (ΔG_{ads}) were negative and ranges between -17 to -9 kJ/mol. This indicates that the adsorption process of the leaves extract is both spontaneous and physical. The notable inhibition efficiency values obtained

from the weight-loss, EIS and PDP experiments revealed that the leaves extract could be recommended for use as a corrosion inhibitor of low carbon steel pipes in a saline environment.

AUTHOR CONTRIBUTIONS

K. D. Ogwo: Conceptualization, Methodology, Weight loss experiment, Writing-original draft, Validation.

L. A. Nnanna: Electrochemical measurements, Supervision, Writing-review and editing.

A. E. Emea: Leaves extraction, Software.

U. Joseph: Software, Writing-review and editing.

A. C. Young: Writing-review and editing.

ACKNOWLEDGEMENT(S)

The authors acknowledged the support of electrochemistry laboratory, Federal University of Technology, Owerri, for making their facilities available for this research.

REFERENCES

E. Akpan (2022). Environmental consequences of oil spills on marine habitats and the mitigating measures: The Niger Delta Perspective, *Journal of Geoscience and Environmental Protection*, 10(6), 191-203. doi:10.4236/gep.2022.106012.

A.A. Al-Amiery; R.W. Isahak and W.K. Al-Azzawi (2023). Corrosion inhibitors: Natural and synthetic organic inhibitors. *Lubricants*, 11(4), 174.

N. Ayawei; N. Augustus and D. Wankasi (2017). Modelling and interpretation of adsorption isotherms. *Journal of Chemistry*, 1, 3039817 https://doi.org/10.1155/2017/3039817

M. Bouguezzi; J. Scheid; D. Hilhorst; H. Matano; C. Bataillon; F. Lequien and F. Rouillard (2024). Anodic dissolution model with diffusion-migration transport for simulating localized corrosion. *Electrochimica Acta*, 477, 143806. doi.org/10.1016/j.electacta.2024.143806

F. Cao; J. Wang; Y. Lian; Y. Wang; X. Wang; A. Song and L. Shi (2024). A study on the influence of the electroplating process on the corrosion resistance of zinc-based alloy coatings. *Coatings*, 13(10), 1774.

H. Casteneda and D.X. Benetton (2008). SRB-biofilm influence in active corrosive sites formed at the steel-electrolyte interface when exposed to artificial seawater conditions. *Corrosion Science,* 50, 169-1183.

S. Chaudhary and R.K. Tak (2022). Natural Corrosion inhibition and adsorption characteristics of *tribulus terrestris* plant extract on aluminium in hydrochloric acid environment. *Biointerface research in applied chemistry*, 12(2), 2603-2617.

A.M. Chidiebere; L. Nnanna; C. Blessing; K. Oguzie; O. Beluonwu; O. Benedict and E. Oguzie (2016). Inhibition of Acid Corrosion of Mild Steel Using *Delonix regia* Leaves. *International letters of chemistry, physics and astronomy*, 69, 74-86.

S. Devikala; P. Kamaraj; M. Arthanareeswari and M.B. Patel (2019). Green corrosion inhibition of mild steel by aqueous *allium sativum* extract in 3.5% NaCl. *Material Today Proceeding,* 14: 580-589

O.A. Ezzat; S.V. Aigbodion; A.H. Al-lohedan and J.C. Ozoude (2024). Unveiling the corrosion inhibition efficacy and stability of silver nanoparticles synthesized using *anacardium occidentale* leaf extract for mild steel in a simulated seawater solution. *RSC Advances*, 14(26), 18395-18405.

M.C. Fatah; A. Diaz and A. Darwin (2019). Corrosion assessment of a leakage pipeline in the seabed: A case study. 4th Annual Applied Science and Engineering Conference. *Journal of Physics: Conference series,* 1402 066001.

S. Feliu (2020). Electrochemical impedance spectroscopy for the measurement of the corrosion rate of magnesium alloys: Brief review and challenges. *Metals*, 10(6), 775. https://doi.org/10.3390/met10060775

K. George (2022). Corrosion barrier coatings: Progress and perspectives of the chemical route. *Corrosion Material Degradation*, 3(3), 376-413.

R. Haldhar; D. Prasad; D. Kamboj; S. Kaya; O. Dagdag and L. Guo (2021). Corrosion inhibition, surface adsorption and computational studies of *Momordica charantia* extract: A sustainable and green approach. *SN Applied Sciences*, 3, 25. Doi.org/10.1007/s42452-020-04079-x

Hussein, F. M., Ben, M. S., Taiwo, R., and Tarek, Z. (2023). Analysis and ranking of corrosion causes for water pipelines: A critical review. *NPJ Clean Water*. doi.org/10.1038/s41545-023-00275-5

G.H. Ibrahim; M. Abdelmotelb; S.M. Elnouby and M.A. Mostafa (2023). Studies on the impact for pyrimidine compounds upon aluminium protection in acidic conditions, both experimentally and theoretically. *Egyptian Journal of Chemistry*, 66(12), 367 – 378.

A.G. Ingale and A.U. Hivrale (2010). Pharmacological studies of Passiflora and their bioactive compounds. *African Journal of Plant Sciences*. 4, 417 – 426.

G. Jeanmairet; B. Rotenberg and M. Salanne (2022). Microscopic simulations of electrochemical double-layer capacitors. *Chemical Reviews*, 122(12), 10860-10898.

S.R. Kachel; B.P. Klein; M.J. Morbec; M. Schöniger; M. Hutter; M. Schmid and G.J. Michael (2020). Chemisorption and Physisorption at the Metal/Organic Interface: Bond Energies of Naphthalene and Azulene on Coinage Metal Surfaces. *Journal of Physical Chemistry*, 8257 - 8268. https://doi.org/10.1021/acs.jpcc.0c00915

H.G. Kalada; O.K. Orubite and O.A. James (2017). Corrosion inhibition of mild steel in simulated seawater by *nymphae pubens* leaf extracts. *International Journal of Advanced Research in Chemical Science,* 4(12), 32-40.

L. Lai; B. Xie; L. Zou; X. Zheng; X. Ma and S. Zhu (2017). Adsorption and corrosion inhibition of mild steel in hydrochloric acid solution by S-allyl-O,O-dialkyldithiophosphates. *Results in Physics*, 7, 3434-3443.

Y. Li; D. Zhang and J. Wu (2010). Study on kinetics of cathodic reduction of dissolved oxygen in 3.5% sodium chloride solution. *Journal of Ocean University of China*, 9, 239-243.

M. Liu; J. Zhu; V.A. Popovich; E. Borisov; M.J. Mol and Y. Gonzalez-Garcia (2023). Passive film formation and corrosion resistance of laser-powder bed fusion fabricated NiTi shape memory alloys. *Journal of Materials Research and Technology*, 23, 2991-3006.

T.J. McGenity; D.B. Folwell; A.B. McKew and G.O. Sanni (2012). Marine Crude oil Biodegradation: A Central role for interspecies interaction. *Aquatic Biosystems*, 8(10), 1-19

A. Menga; T. Kanstad; D. Cantero; L. Bathen; K. Hornbostel and A. Klausen (2022). Corrosion induced damges and failures of post-tensioned bridges: A literature review. *Structural Concrete,* 24(1), 84-99. https://doi.org/10.1002/suco.202200297

M. Mobin and S. Zehra (2023). Electrochemical and analytical techniques for sustainable corrosion monitoring: Corrosion control by cathodic protection. *Advances, Challenges and Opportunities*, 265-279.

A.F. Nunez (2024). Electrochemical analysis of corrosion resistance of manganese-coated annealed steel: Chronoamperometric and voltametric study. *Applied Chem*istry, 4(4), 367-383.

K.D. Ogwo; L. Nnanna; Y. Ahamefule and E.A. Emea (2024a).
Comparative Investigation of the corrosion protection efficacy of *Spondias mombin* leaf extracts on AA2024 alloy and low carbon steel in acidic medium. *Physical Science International Journal,* 28(3), 13-23.

K.D. Ogwo; L. Nnanna; C.A. Young and U. Joseph (2024b). Corrosion mitigation effect of green inhibitor on aluminium alloy (AA2024) in 3.5wt. % NaCl. *Proceedings of the maiden research and innovation fair/conference*, Michael Okpara University of Agriculture, Umudike, 766-772, Nigeria.

K.D. Ogwo; L. Nnanna; U.C. Onyeije and A.D. Asiegbu (2023). Electrochemical Investigation of the Anti-corrosive Effect of *Spondias mombin* Leaves Extract on the Corrosion of Aluminium Alloy (AA2024) and Mild Steel in 0.5 M NaCl. *Chemical Science International Journal,* 32(3), 44-51.

Othman, N. K., Yahya, S., and Ismail, C. M. (2019). Corrosion inhibition of steel in 3.5% NaCl by rice straw extract. *Journal of Industrial Engineering & Chemistry*, 70, 299-310.

K. Paswan; S. Sharma; P.D. Shashi; M.K. Abdulameer; L. Changhe; Y. Yaser; M. Abbas and E. Tag-Eldin (2023). An analysis of microstructural morphology, surface topography, surface integrity, recast layer, and machining performance of graphene nanosheets on Inconel 718 superalloy: Investigating the impact on EDM characteristics, surface characterizations, and optimization. *Journal of Materials Research and Technology*, 27, 7138 – 7158.

K.V. Rybalka; L.A. Beketaeva and D.A. Davydov (2021). Estimation of corrosion rate of AISI 1016 steel by the analysis of polarization curves and using the method of measuring ohmic resistance. *Russian Journal of Electrochemistry*, 57, 16-21.

R.B. Sheetal; K.A. Singh; M. Singh; T. Sanjeeve; B. Pani and S. Kaya (2023). Advancement of corrosion inhibitor system through N-heterocyclic compounds: a review. *Corrosion Engineering Science and Technology,* 58(1), 73-101.

K.M. Shwetha; B.M. Praveen and B.K. Devendra (2024). A review on corrosion inhibitors: Types, mechanisms, electrochemical analysis, corrosion rate and efficiency of corrosion inhibitors on mild steel in an acidic environment. *Results in Surfaces and Interfaces,* 16, 100258. doi.org/10.1016/j.rsurfi.2024.100258

R. Solmaz; A. Salci; Y.A. Dursun and G. Kardas (2023). A comprehensive study on the adsorption, corrosion inhibition efficiency and stability of *acriflavine* on mild steel in 1 M HCl solution. *Colloids and Surfaces: A Physicochemical and Engineering Aspects*, 674, 131908. Doi.org/10.1016/j.colsurfa.2023.131908

C. Song; Y. Li; F. Wu; J. Luo; L. Li and G. Li (2023). Failure analysis of the crack and leakage of a crude oil pipeline under CO_2-Steam flooding. *Processes*, 11(5), 1567.

Y. Zhai; X. Guo; Y. He and Z. Li (2023). Corrosion resistance and mechanical properties of electrodeposited Co-W/ZrO_2 composite coatings. *International Journal of Electrochemical Science,* 18(3), 100015. https//doi.org/10.1016/j.ijoes.2023.01.015

A. Zakeri; E. Bahmani and A.S. Aghdam (2022). Plant extracts as sustainable and green corrosion inhibitors for protection of ferrous metals in corrosive media. A mini review. *Corrosion Communications*, 5, 25-38.